Synthesis and Characterization of Clarithromycin-Graphene Oxide for Antibacterial Drug Delivery

Vincentsia V. Vanessa[1] and Julia M. Tan[2*]
[1]School of Biosciences, Taylor's University, No. 1, Jalan Taylor's, Subang Jaya, 47500 Selangor Darul Ehsan, Malaysia
[2]New Energy Science and Chemical Engineering, Xiamen University Malaysia, Jalan Sunsuria, Bandar Sunsuria, 43900 Sepang, Selangor Darul Ehsan, Malaysia
*Corresponding author (e-mail: juliatan@xmu.edu.my)

The conventional oral formulation of the antibacterial drug clarithromycin has always been a major challenging task to overcome due to its low bioavailability, short circulation half-life, poor aqueous solubility, and acidic instability inside the stomach. Therefore, targeted drug delivery system is one of the key solutions to overcome these pharmaceutical limitations. A study was conducted to formulate and optimize the clarithromycin loading efficiency of a novel nanoparticle-mediated drug delivery system based on graphene oxide as the carrier. The clarithromycin-graphene oxide nanohybrid was synthesized using a simple, non-covalent functionalization method and characterized by ultraviolet-visible and Fourier transform infrared spectroscopies. The drug loading efficiency of graphene oxide was estimated to be around 56.0 wt% and the Fourier transform infrared spectra suggested that clarithromycin was successfully conjugated onto graphene oxide as evidenced by the characteristic absorption peaks of both graphene oxide and clarithromycin. The findings herein strongly indicate that graphene oxide, as a multifunctional and versatile nanomaterial, can be a potential drug carrier for enhancing the pharmacokinetic profiles of poorly water-insoluble drugs like clarithromycin.

Key words: Functionalization; antibiotic; bioavailability; nanomedicine; drug delivery system

Received: September 2020; Accepted: October 2020

Clarithromycin (CLM), commonly prescribed in the oral dosage form of tablets, is a semi-synthetic 14-membered lactone ring macrolide derived from erythromycin (ERM) by the substitution of the hydroxyl group at position six with a methoxide group (Figure 1). This macrolide functions via inhibition of bacterial protein synthesis by binding to the larger subunit, 50S, of the bacterial ribosomes. Its active metabolite, 14-(R)-hydroxyclarithromycin (14-OH), can also act synergistically with the parent compound, and thereby further increases the bioavailability of CLM in the intracellular sites. Besides, CLM is listed as one of the safest and most effective essential medicines by the World Health Organization for treating a wide variety of bacterial infections caused by both gram-negative and gram-positive bacteria [1]. Apart from that, this drug can be used concomitantly with acid-suppressing agents to treat stomach ulcers caused by *Helicobacter pylori*, as well as to prevent the growth of *Mycobacterium avium* associated with acquired immunodeficiency syndrome (AIDS) patients [2,3]

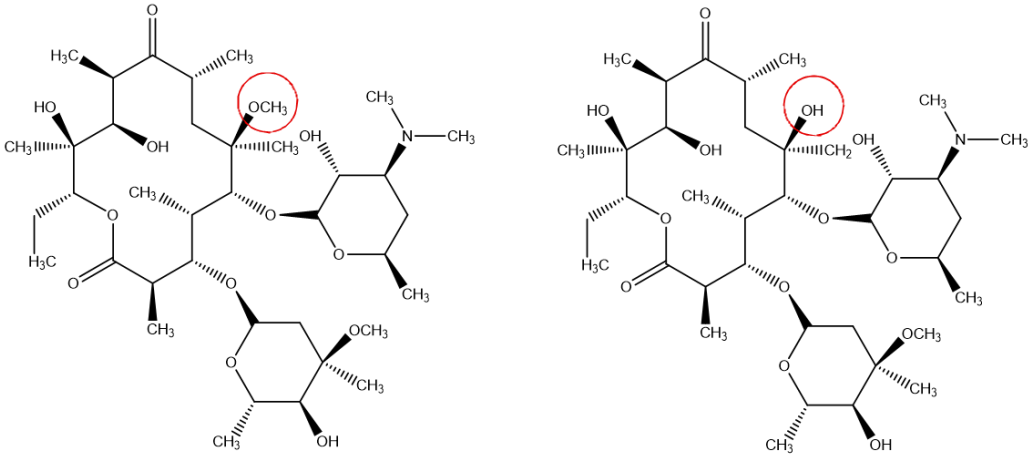

(a) **(b)**

Figure 1. The chemical structures of (a) CLM and (b) ERM.

According to Biopharmaceutical Classification System, CLM is categorized as a class II drug with high membrane permeability but low solubility (around 0.35 μg/mL) in aqueous media [4]. This drug has a substantially low bioavailability (50-55%) due to its poor aqueous solubility characteristic and first-pass effect of the gastrointestinal tract before it reaches the systemic circulation. When CLM is orally administered into the human body, approximately 30-40% of the drug is excreted unchanged or as an active metabolite by the kidneys and the rest is excreted in the bile [5]. As a result, this greatly affects the drug's efficacy, and hence only a small dose of the drug reaches the target site successfully.

To achieve the desired therapeutic outcome and patient compliance, oral administration has always been the most acceptable and preferable route of drug delivery for the systemic circulation due to its non-invasive approach and ease of administration. However, concerns related to CLM's poor pharmacokinetic profiles such as poor solubility in the physiological pH range and low bioavailability *in vivo* have limited its application as an effective antibacterial drug. As such, there is an urgent need to redesign the conventional method of delivering orally administered drugs like CLM through the development of a revolutionary approach - nanotechnology. It is a relatively new terminology used to describe the design, characterization, production, and application conducted at the nanometer scale range, from a few nanometers to much less than 100 nm. The application of nanotechnology in the field of medicine is known as nanomedicine, which involves *in vivo* diagnosis, bioimaging, and targeted drug delivery with the exploitation of a smart, nanoscale-mediated agent (e.g., dendrimers, liposomes, metal nanoparticles, polymeric micelles, carbon nanoparticles, etc).

In the past few decades, extensive work has been rapidly carried out by pharmaceutical scientists on carbon-based nanomaterials, in particular graphene oxide (GO), as novel multifunctional drug delivery agents to improve drug solubility under physiological conditions [6,7]. Graphene oxide, a two-dimensional structure which consists of a monoatomic layer of carbon atoms arranged in the form of a honeycomb network has been regarded as the precursor for all sp^2 graphitic materials with different geometries (Scheme 1). It can be obtained by surface chemical treatment using strong oxidizing agents under acidic conditions to yield oxygen and hydroxyl functional groups with the aim of enhancing its hydrophilicity characteristic. In drug delivery applications, GO exhibits superior qualities when compared to other forms of carbon nanoparticles in terms of lower production cost, better biocompatibility due to absence of toxic metal particles, ease of fabrication and modification as well as demonstrating higher surface area for the immobilization of various bioactive molecules [9]. Therefore, GO is widely researched by scientists around the globe as an effective multifunctional drug delivery platform in recent years for its novelty and versatility in the modern medicine industry.

In this context, the aim of this study was to optimize the formulation of the CLM-GO nanohybrid systematically by investigating multiple independent variables, for instance, the solvent type, GO concentration, sonication period, and reaction time. The nanohybrid was synthesized by a simple method via non-covalent functionalization using ultrasonication and constant-stirring process. The drug loading efficiency of the prepared nanohybrid was then characterized by ultraviolet-visible (UV-vis) spectroscopy and the chemical interaction between CLM and GO was verified by Fourier transform infrared (FTIR) spectroscopy.

EXPERIMENTAL

Chemicals and Materials

A brownish black powdery form of GO (15-20 sheets, 4-10% edge-oxidized) was obtained from Sigma Aldrich (USA). CLM ($C_{38}H_{69}NO_{13}$, molecular weight: 747.95) with a purity of 98% was sourced from Sigma Aldrich (Israel). Acetone (C_3H_6O, molecular weight: 58.08) with a purity of 99.5% was procured from R&M Chemicals (Malaysia). Ethanol (C_2H_5OH, molecular weight: 46.07) with a purity of 99.8% and methanol (CH_3OH, molecular weight: 32.04) with a purity of 99.8% were bought from Merck Millipore (Germany). All other chemicals and solvents were of analytical grade and used as received.

Preparation of clarithromycin stock solutions in methanol, ethanol, and acetone

A stock solution of CLM was prepared by dissolving 8 mg of the drug in 3 mL of methanol and ultra-sonicated until all the drug had fully dissolved. From the stock, the CLM solution was diluted to obtain a series of concentrations ranging from 0.33 mg/mL to 2.00 mg/mL. All dilutions were scanned in the range of 200-700 nm to determine the maximum absorption wavelength, λ_{max}, of CLM (against a blank organic solvent reference) using an UV-vis spectrophotometer and triplicate absorbance readings were obtained for each concentration. The stock solutions of CLM in ethanol and acetone were prepared using a similar method as described. The λ_{max} of CLM was observed to be at 290, 289, and 291 nm for methanol, ethanol and acetone, respectively. Subsequently, standard calibration curves for the three CLM stock solutions were plotted by using the average values obtained from the triplicate absorbance readings to construct a regression line equation in the range of 0.33-2.00 mg/mL.

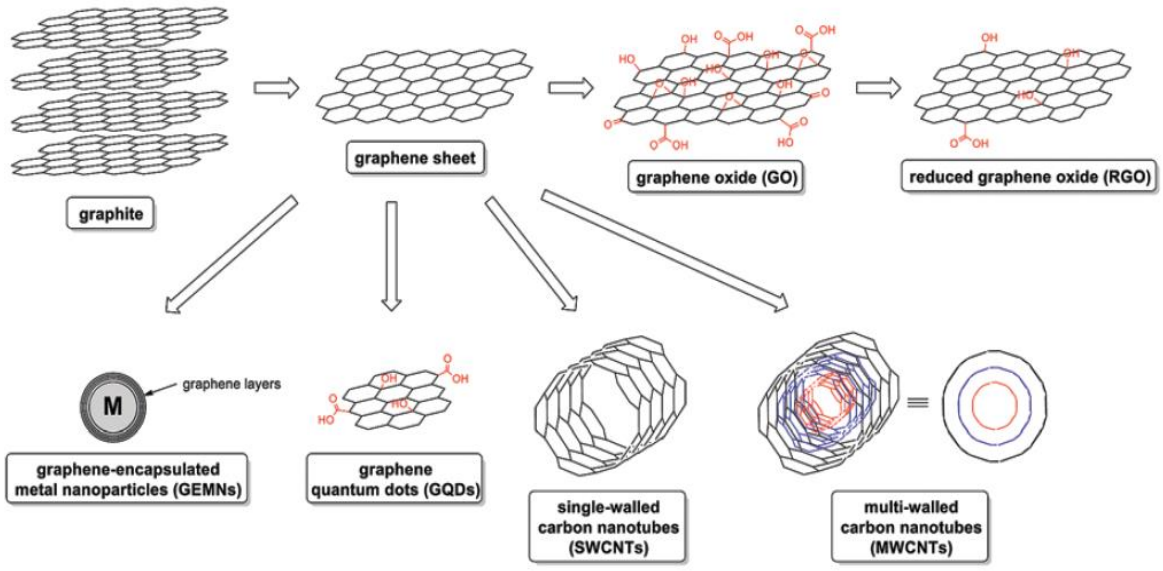

Scheme 1. The illustration of graphitic materials in different forms: (a) flat nanostructures (graphene sheet, graphene oxide, reduced graphene oxide, and graphene quantum dots); (b) tubular nanostructures (single-walled and multi-walled carbon nanotubes); and (c) spherical nanostructures (graphene-encapsulated metal nanoparticles). Taken from Ref. [8] with permission.

Synthesis of CLM-GO based on different masses of graphene oxide

An accurately weighed 150 mg of pure CLM was dissolved in 75 mL of ethanol (2 mg/mL) and the mixture was ultra-sonicated briefly to ensure complete dissolution of the drug. The prepared CLM stock solution was kept at 5˚C in a fridge for the next experiment.

To investigate the drug loading efficiency of GO, the mass of the commercially purchased GO was varied at 2, 4, 6, 8, 10, 15, and 20 mg. A mixture of GO dispersed in 4 mL of the CLM stock solution was prepared with an ultra-bath sonicator at 30–37˚C for 30 minutes. After that, the suspension was placed in an incubator with a speed of 200 rpm at 37˚C for 21 hours to facilitate the attachment of CLM onto GO nanocarrier. Following the drug conjugation process, a black precipitate was obtained after three cycles of washing and centrifugation at 15 000 rpm to remove excess unattached CLM in the supernatant. Finally, the precipitate was dried overnight in an oven at 60˚C to yield CLM-GO nanohybrid. The supernatant was kept for spectrophotometric determination as it still contained an excessive amount of unbound drug. The absorbance of the supernatant was measured at 289 nm, which is the characteristic wavelength of CLM dissolved in ethanol, and calculated according to the following formula:

$$\text{Drug loading efficiency (wt\%)} = \frac{(Weight_{initial\ drug} - Weight_{drug\ in\ supernatant})}{Weight_{initial\ drug}} \quad (1)$$

Synthesis of CLM-GO based on different ultra-sonication times

Briefly, 8 mg of GO (as optimized from the previous experiment) was added to 4 mL of the CLM stock solution prepared separately in a set of seven clean and dry centrifuge tubes. This was followed by a series of different ultra-sonication times at 30, 60, 90, 105, 120, 135, and 150 minutes at a temperature maintained around 30-37˚C. Subsequently, the suspension was then agitated in an incubator (37˚C and 200 rpm) for 21 hours to expedite the drug loading process and subjected to centrifugation at 15 000 rpm for 30 minutes. The supernatant separated from the precipitate was used for the determination of drug loading efficiency, while the precipitate was centrifuged and rinsed with ethanol three times to remove excess unreacted drug. Finally, the precipitate was dried overnight in an oven at 60˚C to obtain CLM-GO nanohybrid.

Synthesis of CLM-GO based on different incubation periods

A total of 80 mg of GO was dispersed in 40 mL of the CLM stock solution followed by ultra-sonication treatment at 30-37˚C for 135 minutes in a bath sonicator. Next, the dispersion was subjected to vigorous shaking at the speed of 200 rpm, while

maintaining the temperature at 37˚C for a series of different incubation periods (7, 8, 10, 12, 14, 16, 18, 20, 21, and 28 hours). The final product, denoted as CLM-GO, was collected and dried using a similar method as described above. The supernatant after centrifugation was analyzed using an UV-vis spectrophotometer and the drug loading efficiency of GO was calculated according to Formula 1.

Characterization Method

An UV-vis spectrophotometer (Lambda XLS, Perkin Elmer Inc., USA) was used to measure the absorption wavelength of GO in the drug loading optimization experiments. The chemical structures of the samples were determined using a Fourier transform infrared spectrophotometer (Spectrum 100 Optica, Perkin Elmer Inc., USA) and scanned in the range from 4000 to 650 cm^{-1}. For FTIR analysis, the samples were prepared by grinding with spectroscopic grade potassium bromide (KBr) powder at the ratio of 1:99 and then pressed into pellets using a special mold and a hydraulic press.

Statistical Analysis

All data were analyzed using IBM SPSS Statistics version 25.0 (USA). One-way analysis of variance (ANOVA) and Tukey HSD test were used to statistically analyze the drug loading efficiency with different ultra-sonication times. Statistical analysis for the drug loading efficiency with different masses of GO and different conjugation periods was performed by Dunnett T3 test. All data were expressed as mean ± standard deviation. Differences between the groups were considered statistically significant at $p < 0.05$.

RESULTS AND DISCUSSION

Characterization

Solubility of CLM in methanol, ethanol and acetone

Based on the UV-vis spectra obtained, a standard calibration curve for each of the three CLM solutions was plotted and is demonstrated in Figure 2. It was observed that CLM dissolved in ethanol best fitted the regression equation with the highest correlation coefficient (R^2) value of 0.9975, which follows Beer-Lambert law. This indicates that there was a significant relationship between the concentration of CLM in ethanol and its absorbance value.

The findings are in accordance to a comparative study conducted by a group of scientists on the lipid extraction using thirteen types of organic solvents [10]. They found that the highest efficiency was achieved by extraction with ethanol, followed by methanol and lastly acetone. Since CLM used in this study is a lipophilic compound, it dissolved well in ethanol compared to methanol. Even though both alcohols are quite efficient in dissolving the pure drug, higher dose of methanol is chemically more toxic than ethanol. This is because methanol is osmotically active in the human body and rapidly metabolized into formic acid, which can further lead to metabolic acidosis and end-organ toxicity, resulting in the damage of retinal and possibly other neurological disturbances [11]. Therefore, ethanol was selected as the preferred solvent for the preparation of the CLM stock solution to be used in the subsequent experiments.

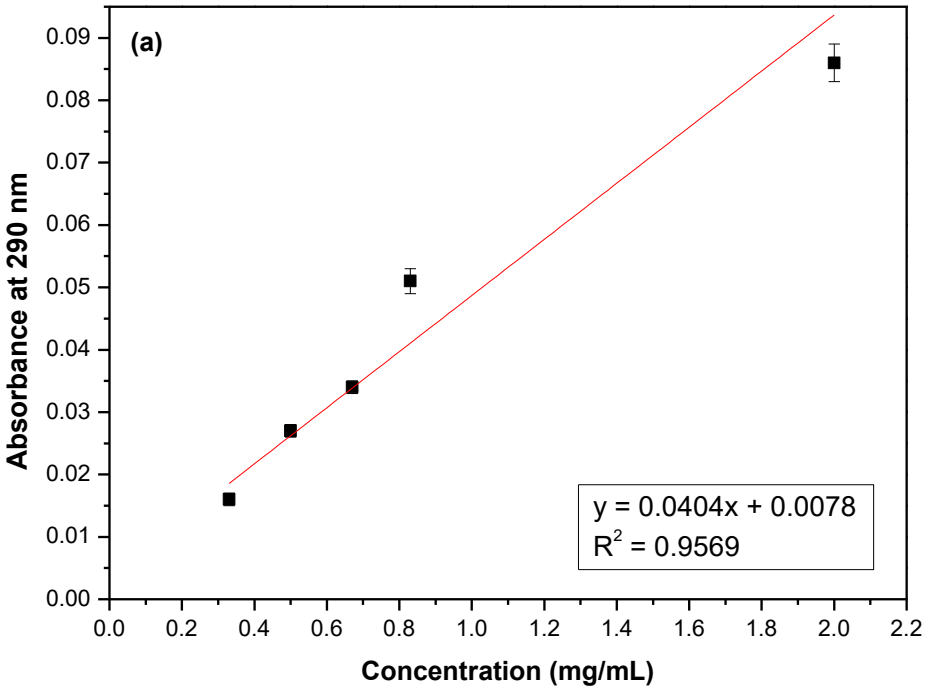

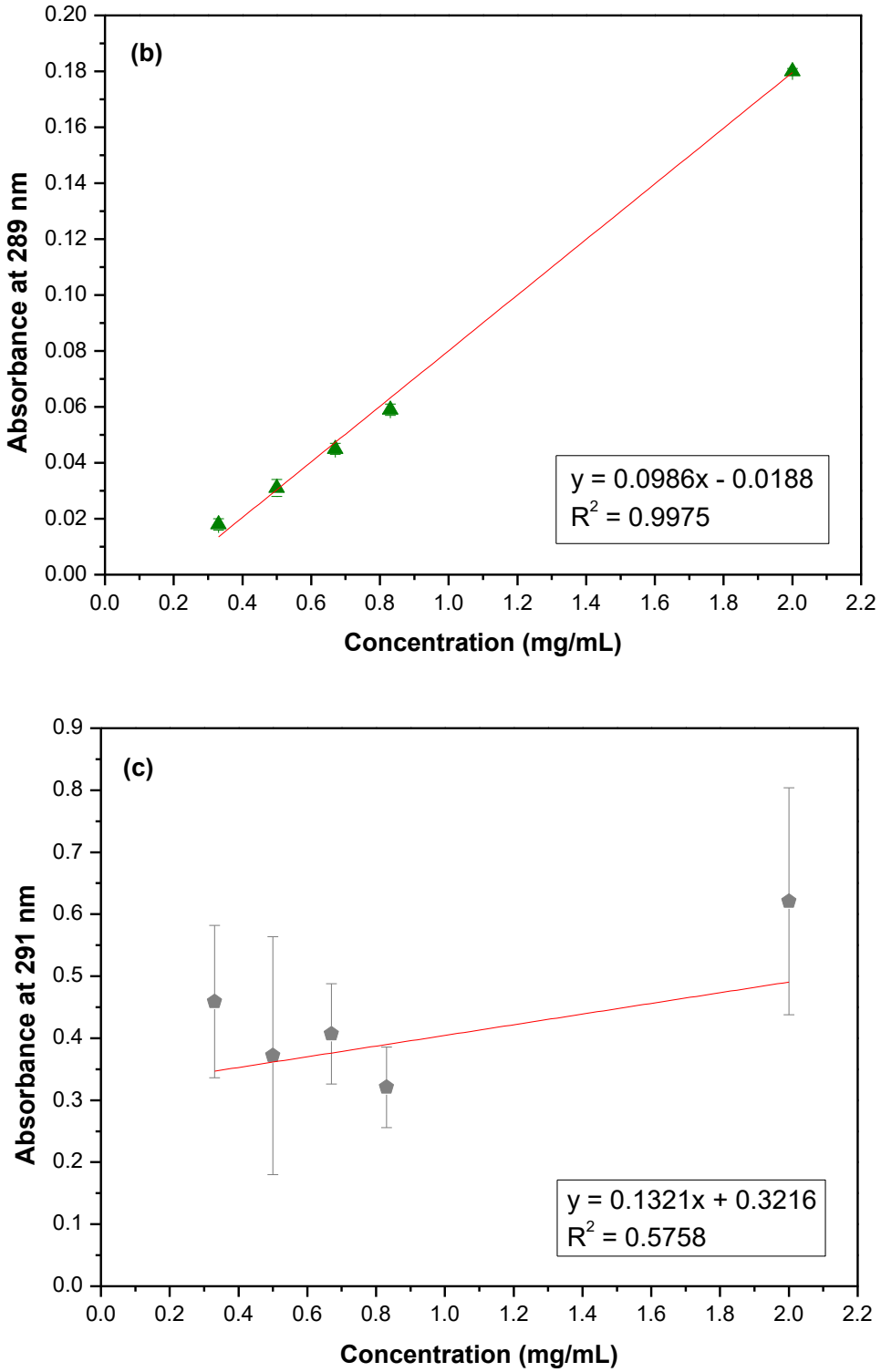

Figure 2. Calibration curves of CLM dissolved in three different organic solvents: (a) methanol, (b) ethanol and (c) acetone, where *y* is the absorbance and *x* is the CLM concentration. Error bars represent standard deviation values of triplicate absorbance readings ($n = 3$).

Evaluation of GO mass on drug loading efficiency

After the conjugation process, unbound CLM left in the supernatant could be used to quantitatively calculate the drug loading efficiency (wt%) with reference to the regression equation and Formula 1.

As shown in Figure 3, the drug loading efficiency of GO increased from the initial value of 36.9 wt% to the highest efficiency of 48.8 wt%, which was achieved by using 8 mg of GO. This phenomenon could be explained by the formation of hydrogen bonds and hydrophobic interactions between individual GO

nanosheets and CLM molecules. GO is normally synthesized according to Hummers method by oxidizing graphite in concentrated sulfuric acid with potassium permanganate [12]. Hence, it acquires its hydrophilic property through the grafting of epoxides, phenols, hydroxyl, carbonyl, and carboxyl functional groups onto its basal planes as well as the edges of the nanosheets [13]. These oxygenated groups are able to attract and intercalate CLM molecules into the layered sheets of stacked-GO, which result in the increase of the loading efficiency.

However, the loading efficiency fell to 45.6 wt% when the mass of GO increased to 10 mg and further decreased to 40.7 wt% at the maximum mass of 20 mg. This finding is consistent with a study conducted on the adsorption effect of an anticancer drug onto GO which was measured in different concentrations, ranging from 0.25 to 0.5 g/L [14]. The authors observed a declining fashion of the adsorption capacity of GO with increasing dosage concentration used in the study. This is because with further increase in the amount of GO, the effective adsorption sites will reduce as a result of partial agglomeration of GO due to van der Waals forces, leading to the decrease of loading efficiency. Therefore, our result suggested that the optimum mass for GO to adsorb CLM in further optimization experiments is 8 mg.

Evaluation of ultra-sonication time on drug loading efficiency

Figure 4 demonstrates that the loading efficiency weightage of GO increased steadily from 37.1% (after 30 minutes of sonication) to a maximum value of 53.7% (after 135 minutes of sonication). Subsequently, the loading efficiency weightage was found to decrease considerably to 43.2% when the sonication time of the sample increased to 150 minutes. The result showed that sonication treatment of GO has a great impact on the loading efficiency and further prolonging the process could lead to the impairment of the GO adsorption capacity. This finding is in good agreement with a study performed on the ultra-sonication of GO and its performance for adsorption applications [15]. The scientists discovered that the adsorption capacity of GO decreased significantly (approximately 75%) after the sample was sonicated up to 120 minutes due to partial removal of oxygen functional groups from GO.

Due to the strong van der Waal cohesive forces, GO is easily agglomerated into closely stacked nanosheets. Thus, in order to achieve a better dispersion state, ultra-sonic treatment is widely applied to break down GO agglomerates and physically separate the stacked layers from each other [16]. Even though this mechanical approach is quite effective in enhancing the homogeneous distribution of GO, intense continuous sonication may break the GO sheets into smaller fragments, and hence decreases its loading efficiency [17]. Besides, fragmentation not only decreases the aspect ratio of GO excessively, but also introduces defective sites in the GO sheets as well as impairs its strengthening roles [18,19]. As such, in order to synthesize an efficient drug carrier for CLM, we adopted 135 minutes as the optimum sonication time in the next section of the study.

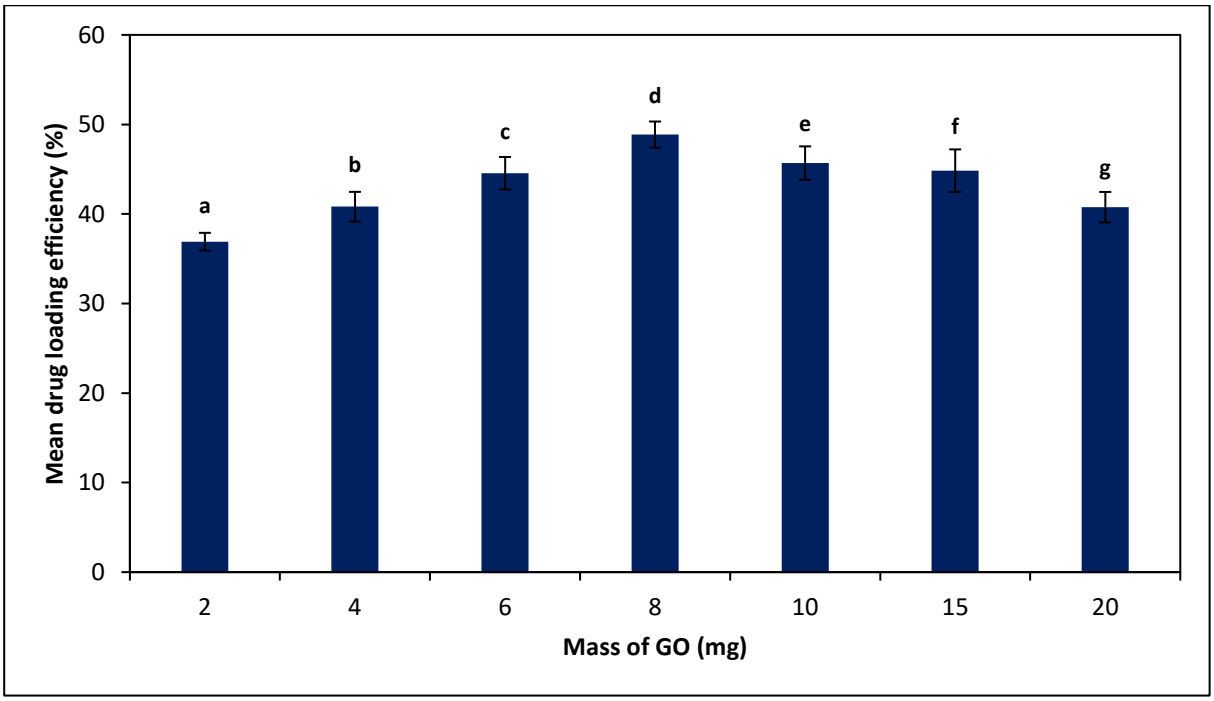

Figure 3. The CLM loading efficiency of GO measured at 289 nm using an UV-vis spectrophotometer. Different alphabets indicate statistically significant differences of the drug loading efficiency between the different masses of GO studied ($n = 9$, $p < 0.05$, ANOVA: Dunnett T3 multiple comparisons).

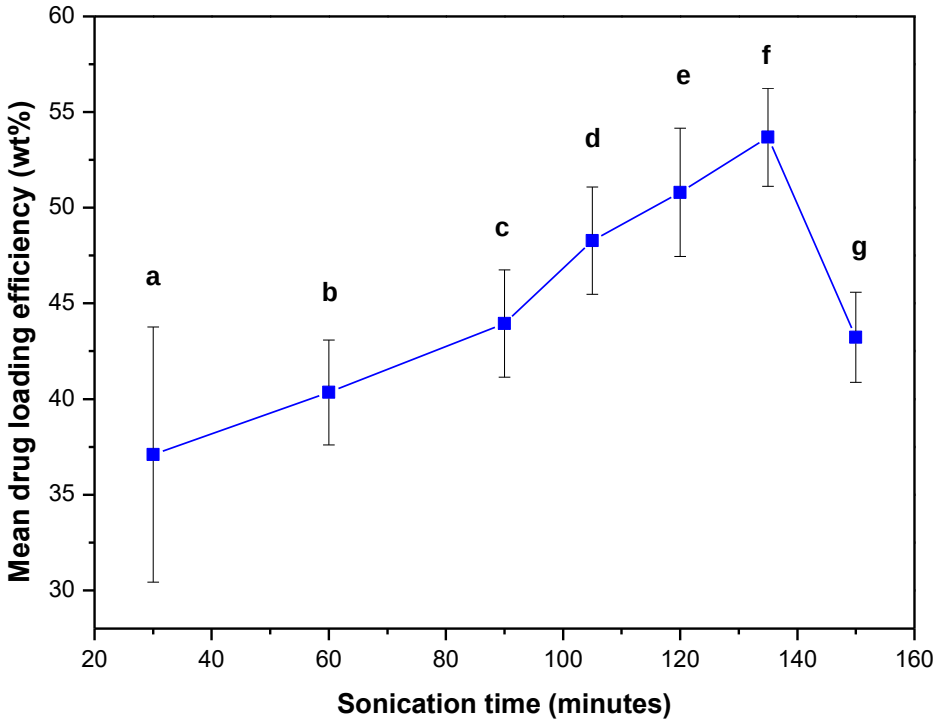

Figure 4. The sonication time of CLM-GO nanohybrid with its respective mean drug loading efficiency and standard deviation. Different alphabets indicate statistically significant differences of the drug loading efficiency determined at different sonication time (n = 9, p < 0.05, ANOVA: Tukey HSD post-hoc test).

Evaluation of conjugation time on drug loading efficiency

Reaction time is one of the critical parameters for the investigation of drug loading process by the drug delivery carrier. From the study, it could be observed that the drug loading efficiency increased gradually with increasing period of reaction time, as depicted in Figure 5. The highest efficiency of drug conjugation was achieved at 56.0 wt% when the sample was incubated and agitated for 18 hours of reaction time. This could be related to the unique one-atom-thick carbon structure of GO where the CLM molecules were attracted to with high force towards the active adsorption sites via oxygenated functional groups [14].

Subsequently, the loading efficiency of GO was found to decrease significantly to 26.3 wt% when the reaction time exceeded 28 hours, indicating that the loading capability of GO had reached its saturation point. The observation was attributed to the decrease of the remaining adsorption sites on the surface of GO after a prolonged incubation period with CLM. Therefore, it caused a declining trend in the adsorption driving force, which eventually lead to a relatively longer time for GO to reach adsorption equilibrium. Based on the statistical analysis, even though the drug loading efficiency of GO was the highest at the reaction time of 18 hours, the sample mean was not significant because p > 0.05. Hence, in order to produce optimum saturated loading efficiency for CLM, reaction time between 14-20 hours would be the best option.

FTIR Characterization

In order to examine the chemical structures and functional groups of the materials, FTIR spectroscopy was used to study the drug-carrier interaction in the optimized formulation as compared to the pure drug and carrier. As shown in Figure 6(a), several intense characteristic absorption peaks were observed in the FTIR spectrum of pure CLM due to the presence of ether, lactone, hydroxyl, carbonyl, ketone, and tertiary amine functional groups [20,21]. The sharp peaks found at 1173, 1052, and 1011 cm^{-1} were attributed to the C-O-C stretching vibration of ether, whereas the strong absorption peaks centered at 1726 and 1581 cm^{-1} were due to the ketone carbonyl stretch of the lactone ring. Apart from that, some relatively weak peaks related to the N-CH_3 stretching vibration in the lactone ring and the aliphatic-CH_2 stretching vibration were seen at 1457 and 1380 cm^{-1}, respectively. Other typical peaks at 3463, 2978, 2941, and 2831 cm^{-1} were assigned to the O-H stretching vibration of hydrogen bond generated between the hydroxyl groups, N-H stretching vibration of the tertiary amine group as well as C-H asymmetric and symmetric stretching vibration of the alkyl-CH_3 group, respectively.

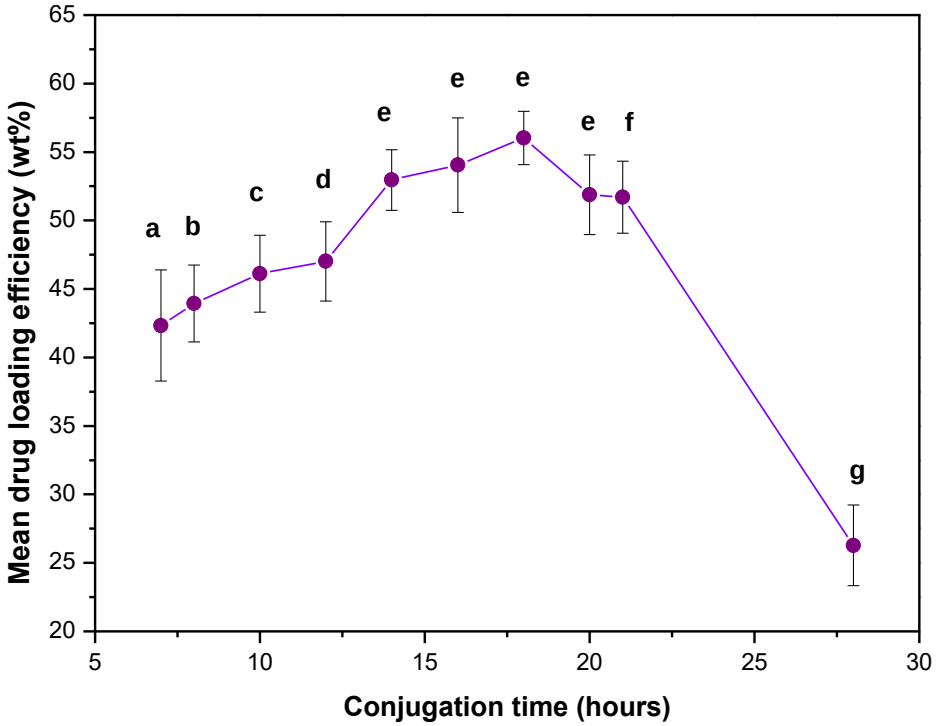

Figure 5. The conjugation time of CLM-GO nanohybrid with its respective mean drug loading efficiency and standard deviation. Different alphabets indicate statistically significant differences of the drug loading efficiency measured at different reaction periods ($n = 9$, $p < 0.05$, ANOVA: Dunnett T3 multiple comparisons).

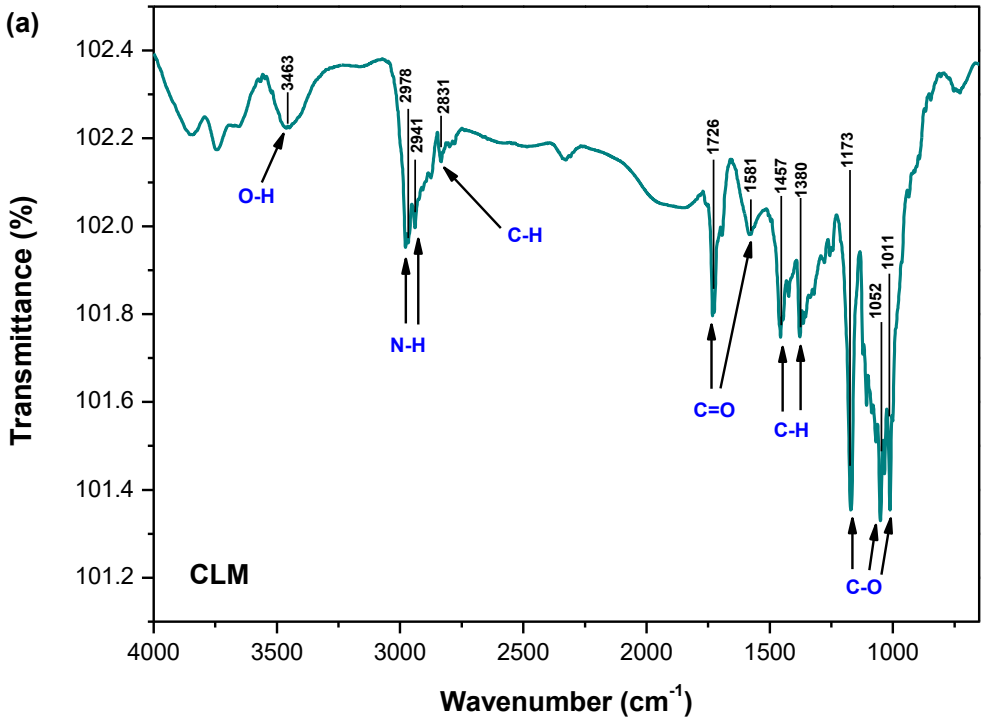

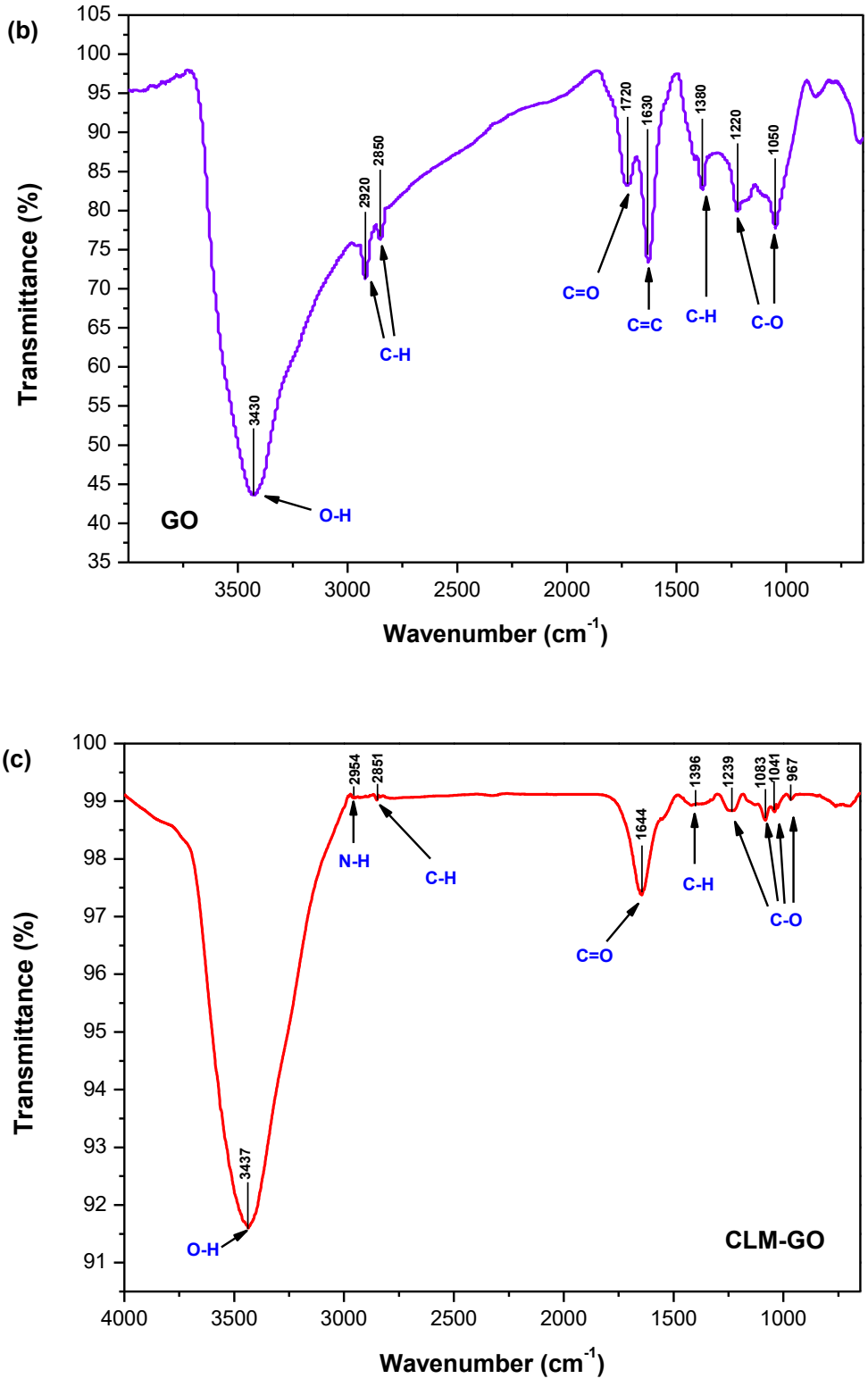

Figure 6. FTIR spectra of (a) pure CLM, (b) commercially purchased GO, and (c) synthesized CLM-GO nanohybrid.

The FTIR spectrum of GO showed numerous intense characteristic absorption peaks, as indicated in Figure 6(b) [22,23]. For example, a broad peak of the O-H stretching vibration was observed at 3430 cm^{-1}, the C-O (epoxy) stretching vibration at 1220 cm^{-1}, and the C-O (alkoxy) stretching vibration at 1050 cm^{-1}. Besides, a moderate peak detected at 1720 cm^{-1} confirmed the presence of the ketone group, and lastly

the peak centered at 1630 cm^{-1} was associated with the skeletal structure of the benzene ring in the GO nanosheet.

Majority of the CLM characteristic absorption peaks were detected in the FTIR spectrum of CLM-GO nanohybrid (Figure 6(c)), indicating the successful loading of CLM onto GO. It was noted that some of the peaks were slightly shifted to lower wavenumber regions due to the drug conjugation process. For instance, the position of the peaks centered at 3463 cm^{-1} (from CLM) and 3430 cm^{-1} (from GO) due to the O-H stretch could have been combined and shifted to 3437 cm^{-1}. On the other hand, the carbonyl absorption peak became more intense and shifted to 1644 cm^{-1} due to overlapping carbonyl vibrations of CLM and GO. It was also interesting to note that several new peaks were recorded at 2954, 2851, 1083, 1041, and 967 cm^{-1}. This observation might be associated with the N-H stretching vibration of the tertiary amine group, C-H stretching vibration of the alkyl aliphatic group, and C-O-C stretching vibration of the ether group, as a result of the non-covalent functionalization of CLM.

Based on the FTIR findings, the formation of CLM-GO nanohybrid was verified and a possible mechanism of CLM attachment onto GO is illustrated in Scheme 2. The unique architecture of GO, which consists of one-atom-thick layered sheet in a two dimensional honeycomb lattice offers an excellent exposure for every carbon atom to be in close contact with the CLM molecules during the conjugation process. Furthermore, the abundant availability of oxygen-containing functional groups, such as carboxyl and hydroxyl groups, positioned at the edge of GO renders it to be more effective for the attachment of CLM through the formation of hydrogen bonding. Therefore, we postulated that the hydrogen bond interaction between CLM and GO may occur in two possible ways: (i) OH group of GO and OH group of CLM and/or (ii) COOH group of GO and OH group of CLM.

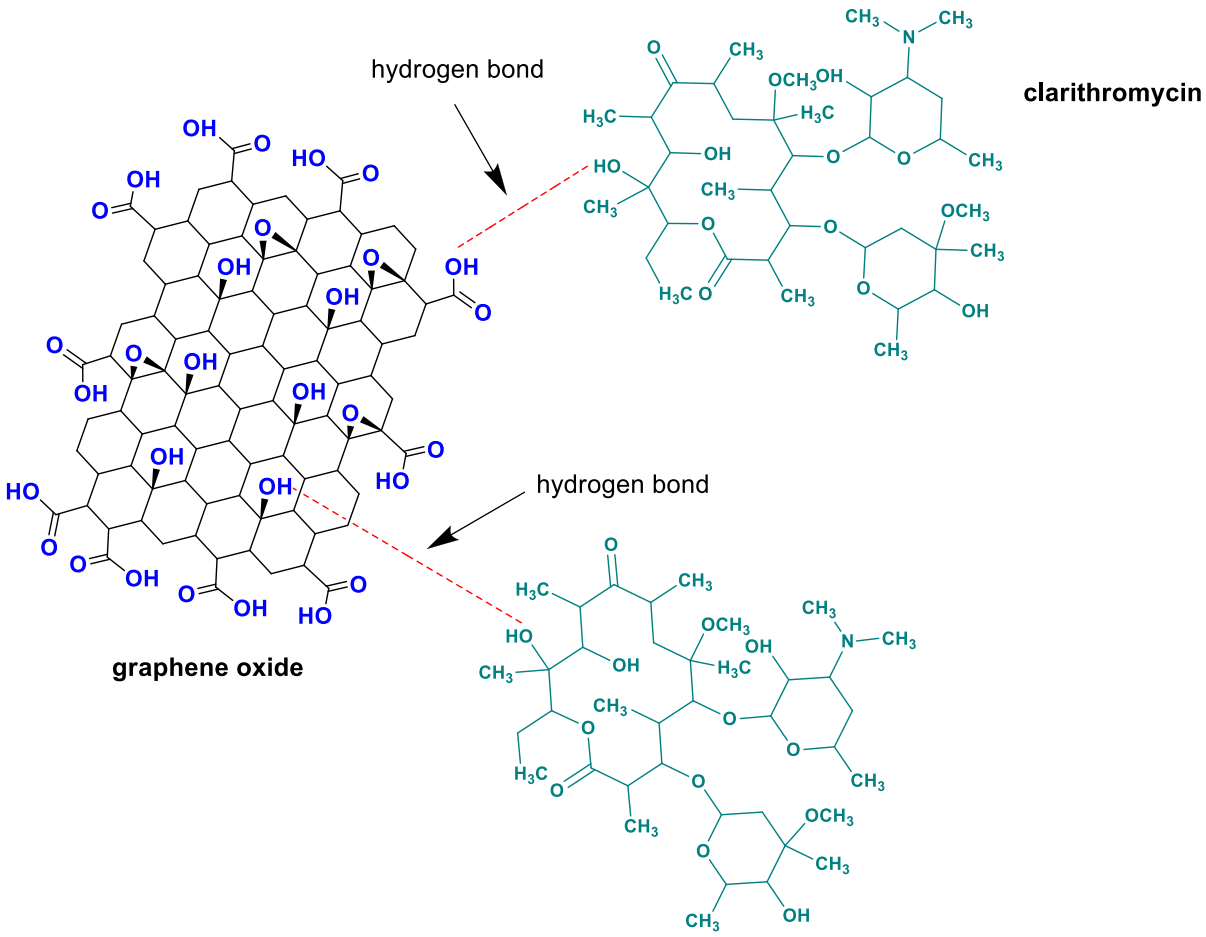

Scheme 2. A schematic drawing of the proposed non-covalent attachment of CLM onto GO via hydrogen bond interaction. The CLM molecules can be loaded on both sides of the GO sheet.

CONCLUSION

In summary, we have prepared an optimized CLM-GO nanohybrid with a relatively high loading efficiency of up to 56.0 wt% by utilizing only a small amount of the nanocarrier (~8 mg). Besides, it was found that ethanol was the most compatible solvent to be used for the drug dissolution where it demonstrated good linearity with a correlation coefficient of 0.9975. FTIR results showed that CLM can be successfully formulated for antibacterial drug delivery with the conjugation of GO through the formation of hydrogen bond and hydrophobic interaction. Despite the promising results, an extensive investigation of the work remains to be done, including the drug release behavior in physiological environment and possible *in vitro* cytotoxicity effects of the synthesized nanohybrid, before it could be utilized in the human body.

ACKNOWLEDGEMENTS

The authors are grateful to Taylor's University School of Biosciences for supporting this research under Final Year Project general funding scheme.

Conflict of Interests

The authors declare that there is no conflict of interests regarding the publication of this paper.

Data Availability

All data generated or analyzed during this study are in cluded in the Supplementary Information.

REFERENCES

1. World Health Organization. Geneva: World Health Organization. Available from: https://apps.who.int/iris/handle/10665/325771.

2. Rajinikanth, P. S. and Mishra, B. (2009) Stomach-site specific drug delivery system of clarithromycin for eradication of *Helicobacter pylori*. *Chemical and Pharmaceutical Bulletin*, **57**, 1068–1075.

3. Zukerman, J. M. (2004) Macrolides and ketolides: azithromycin, clarithromycin, telithromycin. *Infectious Disease Clinics of North America*, **18**, 621–649.

4. Esfandi, E., Ramezani, V., Vatanara, A., Najafabadi, A. R. and Moghaddam, S. P. H. (2014) Clarithromycin dissolution enhancement by preparation of aqueous nanosuspensions using sonoprecipitation technique. *Iran Journal of Pharmaceutical Research*, **13**, 809–818.

5. Hardy, D. J., Guay, D. R. P. and Jones, R. N. (1992) Clarithromycin, a unique macrolide: A pharmacokinetic, microbiological, and clinical overview. *Diagnostic Microbiology and Infectious Disease*, **15**, 39–53.

6. Liu, Z., Robinson, J. T., Sun, X. and Dai, H. (2008) PEGylated nanographene oxide for delivery of water-insoluble cancer drugs. *Journal of the American Chemical Society*, **130**, 10876–10877.

7. McCallion, C., Burthem, J., Rees-Unwin, K., Golovanov, A. and Pluen, A. (2016) Graphene in therapeutics delivery: problems, solutions and future opportunities. *European Journal of Pharmaceutics and Biopharmaceutics*, **104**, 235–250.

8. Kasprzak, A. and Poplawska, M. (2018) Recent developments in the synthesis and applications of graphene-family materials functionalized with cyclodextrins. *Chemical Communications*, **54**, 8547–8562.

9. Geim, A. K. and Novoselov, K. S. (2007) The rise of graphene. *Nature Materials*, **6**, 183–191.

10. Liu, J., Cui, L. and Losic, D. (2013) Graphene and graphene oxide as new nanocarriers for drug delivery applications. *Acta Biomaterialia*, **9**, 9243–9257.

11. Ramluckan, K., Moodley, K. G. and Bux, F. (2014) An evaluation of the efficacy of using selected solvents for the extractionof lipids from algal biomass by the soxhlet extraction method. *Fuel*, **116**, 103–108.

12. Ashurst, J. V. and Nappe, T. M. (2020) In *StatPearls [Internet]*; Treasure Island: StatPearls Publishing, FL. *Available from:* https://www.*ncbi.nlm.nih.gov/books/NBK482121/*.

13. Hummers Jr., W. S. and Offeman, R. E. (1958) Preparation of graphitic oxide. *Journal of the American Chemical Society*, **80**, 1339.

14. Shareena, T. P. D., McShan, D., Dasmahapatra, A. K. and Tchounwou, P. B. (2018) A Review on graphene-based nanomaterials in biomedical applications and risks in environment and health. *Nano-Micro Letters*, **10**, https://doi.org/10.1007/s40820-018-0206-4.

15. Wu, S., Zhao, X., Li, Y., Du, Q., Sun, J., Wang, Y., Wang, X., Xia, Y., Wang, Z. and Xia, L. (2013) Adsorption properties of doxorubicin hydrochloride onto graphene oxide: equilibrium, kinetic and thermodynamic studies. *Materials*, **6**, 2026–2042.

16. Le, G. T. T., Chanlek, N., Manyam, J., Opaprakasit, P., Grisdanurak, N. and Sreearunothai, P. (2019) Insight into the

ultrasonication of graphene oxide with strong changes in its properties and performance for adsorption applications. *Chemical Engineering Journal*, **373**, 1212–1222.

17. Ye, S. and Feng, J. (2016) The effect of sonication treatment of graphene oxide on the mechanical properties of the assembled films. *RSC Advances*, **6**, 39681–39687.

18. Baig, Z., Mamat, O., Mustapha, M., Mumtaz, A., Munir, K. S. and Sarfraz, M. (2018) Investigation of tip sonication effects on structural quality of graphene nanoplatelets (GNPs) for superior solvent dispersion. *Ultrasonics Sonochemistry*, **45**, 133–149.

19. Li, Y., Umer, R., Samad, Y. A., Zheng, L. and Liao, K. (2013) The effect of the ultrasonication pre-treatment of graphene oxide (GO) on the mechanical properties of GO/polyvinyl alcohol composites. *Carbon*, **55**, 321–327.

20. Barnard, A. S. and Snook, I. K. (2008) Thermal stability of graphene edge structure and graphene nanoflakes. *The Journal of Chemical Physics*, **128**, 094707.

21. Baibhav, J., Gurpreet, S.; AC, R. and Seema, S. (2012) Development and characterization of clarithromycin emulgel for topical delivery. *International Journal of Drug Development and Research*, **4**, 310–323.

22. Sharma, M., Gupta, N. and Gupta, S. (2016) Implications of designing clarithromycin loaded solid lipid nanoparticles on their pharmacokinetics, antibacterial activity and safety. *RSC Advances*, **6**, 76621–76631.

23. He, D., Peng, Z., Gong, W., Luo, Y., Zhao, P. and Kong, L. (2015) Mechanism of a green graphene oxide reduction with reusable potassium carbonate. *RSC Advances*, **5**, 11966–11972.

24. Rattana, T., Chaiyakun, S., Witit-anun, N., Nuntawong, N., Chindaudom, P., Oaew, S., Kedkeaw, C. and Limsuwan, P. (2012) Preparation and characterization of graphene oxide nanosheets. *Procedia Engineering*, **32**, 759–764.